Available online at www.sciencedirect.com
SCIENCE DIRECT
Polymer 47 (2006) 1995–2000
polymer
www.elsevier.com/locate/polymer

CP/MAS ^{13}C NMR analysis of the structure and hydrogen bonding of melt-crystallized poly(vinyl alcohol) films

Hu Yang [a,1], Shaohua Hu [a,2], Fumitaka Horii [a,*], Ryokei Endo [b], Tetsushi Hayashi [b]

[a] *Institute for Chemical Research, Kyoto University, Uji, Kyoto 611-0011, Japan*
[b] *Kuraray Co., Ltd, Sakazu, Kurashiki, Okayama 710-8622, Japan*

Received 12 October 2005; received in revised form 19 January 2006; accepted 24 January 2006

Abstract

The structure and hydrogen bonding of the melt-crystallized atactic poly(vinyl alcohol) (A-PVA) films, which were carefully prepared without significant thermal degradation, have been characterized by CP/MAS ^{13}C NMR spectroscopy. The ^{13}C spin–lattice relaxation analysis has revealed that there exist three components with different T_{1C} values, the crystalline, less mobile noncrystalline and mobile noncrystalline components, in good accord with the results for different PVA samples previously reported. It should be noted that the T_{1C} values of the crystalline and noncrystalline components are appreciably smaller for the melt-crystallized films than those for the un-annealed and annealed samples prepared by casting from the aqueous solution. The ^{13}C NMR spectra of the crystalline and noncrystalline components are separately recorded by using the difference in T_{1C} and their CH lines are successfully resolved into three and seven constituent lines by the least-squares curve fitting, respectively. Moreover, the statistical analysis of the integrated intensities of the constituent lines thus obtained enables to determine the probability f_a for the formation of intramolecular hydrogen bonding in the successive two OH groups along each chain and another probability f_t of the *trans* conformation for the crystalline and noncrystalline components. It is found that the f_a value is relatively larger for the melt-crystallized films than those for the un-annealed and annealed samples. On the basis of these results, the features of the melt-crystallization and the resulting crystalline–noncrystalline structure are discussed by particularly considering effects of intra- and inter-molecular hydrogen bonding on the crystallization.

Keywords: CP/MAS ^{13}C NMR; Poly(vinyl alcohol); Melt-crystallization

1. Introduction

Poly(vinyl alcohol) (PVA), which is commercially produced on a large scale, is one of water-soluble and environmentally-friendly synthetic polymers and thus it has been utilized in various industrial application fields [1,2]. PVA is semi-crystalline even in an atactic form although the crystallinity is a moderate level. Since the crystallization affects physicochemical and mechanical properties of polymer materials, the crystal structure and morphology composed of the crystalline and noncrystalline phases have also widely been studied for PVA by various techniques [1–5]. In most of these cases, however, PVA was crystallized from the aqueous or nonaqueous solution because the serious thermal degradation of PVA usually occurs during the crystallization from the melt. Recently, Endo et al. [6] reported for the first time that it is possible to crystallize conventional atactic PVA (A-PVA) from the melt without significant thermal degradation by properly controlling the preparation conditions: using A-PVA carefully purified and water instead of dimethyl sulfoxide (DMSO) as a casting solvent for the preparation of the starting films, careful degassing of the films before melting, and melting under a high vacuum. As a result, the films could be maintained in the melt at 250 °C for 30 min and then in the supercooled state at 220 °C for 8 h without appreciable thermal degradation. They successfully prepared the melt-crystallized A-PVA samples by this method and studied the melt-crystallization process and the morphological structure such as spherulites and lamellae in detail. However, the molecular structure including the chain conformation and hydrogen bonding has not been clarified for the crystalline and noncrystalline regions in the melt-crystallized samples, which may be very

* Corresponding author. Tel.: +81 774 38 3150; fax: +81 774 38 3148.
E-mail address: horii@scl.kyoto-u.ac.jp (F. Horii).
[1] On leave from College of chemistry and chemical Engineering Nanjing University, Nanjing, People's Republic of China.
[2] Present address: College of Material and Engineering, Donghua University, Shanhai, People's Republic of China.

0032-3861/$ - see front matter © 2006 Elsevier Ltd. All rights reserved.
doi:10.1016/j.polymer.2006.01.082

important for further understanding of PVA characteristics in scientific and practical application fields.

In the previous investigations [7–15], we have already established the systematic characterization method of the chain conformation and intra- and inter-molecular hydrogen bonding separately in the crystalline and noncrystalline components for different PVA samples by CP/MAS ^{13}C NMR spectroscopy. In particular, by assuming the random distribution of *trans* and *gauche* conformations along the PVA chains and the statistical formation of the intramolecular hydrogen bonds between appropriate adjacent OH groups without employing any crystal structure model, two sorts of probabilities could successfully be obtained for the distribution of the *trans* conformation and for the formation of the intramolecular hydrogen bonding [15]. In this paper, we apply the similar method to the characterization of the structure and hydrogen bonding in the crystalline and noncrystalline regions of the melt-crystallized A-PVA films and compare the results with those of the un-annealed and annealed A-PVA films prepared by casting from the aqueous solution [15].

2. Experimental

2.1. Samples

The A-PVA sample used was provided by Kuraray Co, the degrees of polymerization and saponification were 1750 and 99.9%, respectively. The triad tacticities, which were determined at 50 °C in deuterated dimethyl sulfoxide (DMSO-d_6) by gated scalar decoupling ^{13}C NMR spectroscopy, are as follows: $mm=0.23$, $mr=0.50$, $rr=0.27$. Purification of A-PVA including the removal of residual sodium acetate was carried out with great care before the use for the melt-crystallization [6].

PVA films with a thickness of about 100 μm were prepared by casting an aqueous solution of the A-PVA sample on a glass plate and then drying them at 50 °C for 2 days in a vacuum. The films, which were cut into small pieces, were crystallized at 220 °C for 3 h in a glass tube after melted at 250 °C for 30 min and then quenched to ice-water. The detailed description of the preparation of the melt-crystallized A-PVA films was made in the previous paper [6].

2.2. ^{13}C NMR measurements

Solid-state ^{13}C NMR measurements were performed at room temperature on a Chemagnetics CMX-200 spectrometer operating at a static magnetic field of 4.7 T. ^{1}H and ^{13}C radio frequency field strengths $\gamma B_1/2\pi$ were 69.4 kHz for both CP and dipolar decoupling processes. The CP contact time was 0.8 ms and the recycle time after the acquisition of a free induction decay (FID) was 7 s. Each sample was packed into a 7 mm cylinder-type MAS rotor with an O-ring seal [7,14–16] and further dried at 50 °C for 15–24 h in vacuum, to prevent the absorption of moisture before and during NMR measurements. The MAS rate was about 3.5 kHz. Totally, 400–600 FIDs were accumulated using 4k data points in the frequency range of 10 kHz. ^{13}C chemical shifts relative to tetramethylsilane (Me_4Si) were determined by using the CH_3 line at 17.36 ppm of hexamethylbenzene crystals as an external reference. The CPT1 pulse sequence [17] was used to measure ^{13}C spin–lattice relaxation times (T_{1C}s).

3. Results and discussion

3.1. Solid-state ^{13}C NMR analysis

Fig. 1(a) shows the CP/MAS ^{13}C NMR spectrum of the melt-crystallized A-PVA films, which was measured at room temperature in the dried state. As is well known, the CH resonance line splits into three lines, line I′, II′ and III′, which are mainly composed of the contributions from lines I, II and III in the spectrum of the crystalline component shown in Fig. 1(b) as described later. These latter lines are, respectively, assigned to the CH carbons associated with two, one and no intramolecular hydrogen bond(s) in the triad sequences with the planar zigzag conformation [7–11,14,15,18]. In order to evaluate the structure and hydrogen bonding in the crystalline and noncrystalline regions, the spectra of the crystalline and noncrystalline components should be separately obtained. Therefore, the ^{13}C spin–lattice relaxation process for the sample has been examined at room temperature by the CPT1 pulse sequence [17].

In Fig. 2, the logarithmic peak intensities of line II′ are plotted against the decay time τ for the longitudinal relaxation. The experimental decay curve, indicated by solid circles, is found not to be a single exponential and it has been resolved into plural exponentials with different T_{1C} values by the computer-aided, least-squares method. Since the composite line (solid line) of the three components, which is expressed by: Eq. (1),

$$M(\tau) = \sum_{i=1}^{3} M_i(0)\exp\left(\frac{-\tau}{T_{1Ci}}\right) \quad (1)$$

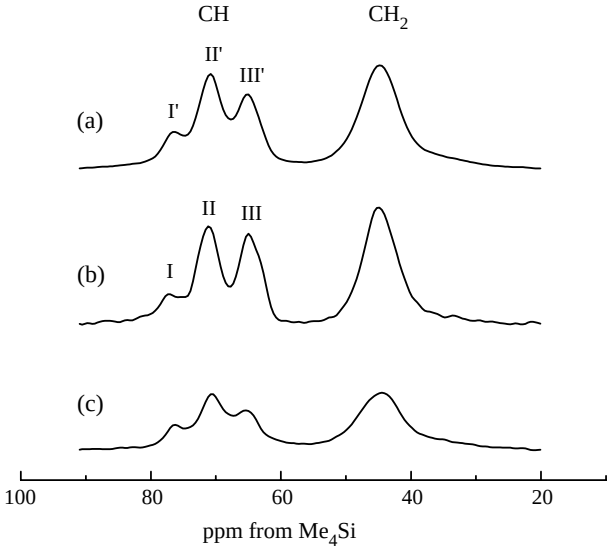

Fig. 1. CP/MAS ^{13}C NMR spectra of different components for the melt-crystallized PVA Films: (a) total, (b) crystalline, (c) noncrystalline ((a)−0.403×(b)). Factor 0.403 was used for the subtraction of the crystalline component (b) from the total spectrum (a).

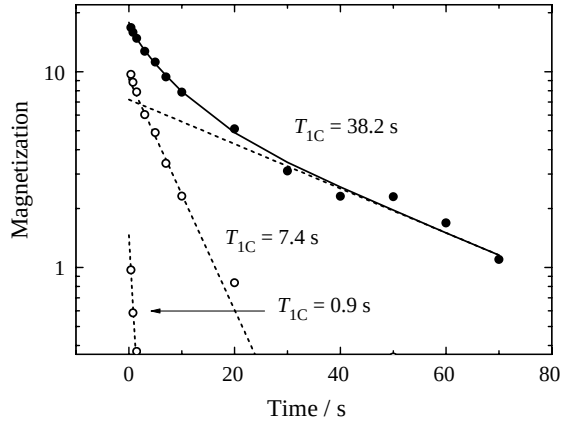

Fig. 2. ^{13}C spin–lattice relaxation process for line II′ of the CH carbons for the melt-crystallized PVA films measured by the CPT1 pulse sequence; solid circles: observed data; open circles: data for each component obtained by subtracting the corresponding longer T_{1C} component(s) from the experimental data. For example, the data for the component with T_{1C}=7.4 s were obtained by subtracting the corresponding values expressed by the broken line for the component with T_{1C}=38.2 s from the observed data; solid line: composite line of the three components; broken line: decay line for each component.

agrees well with the observed data, it should be concluded that there exist three components with different T_{1C} values in good accord with the previous results for various PVA samples [7–11,14,15]. Other resonance lines were also found to contain similar three components and their T_{1C} values are listed in Table 1 together with the previous results for the un-annealed and annealed films, which were prepared at room temperature by casting from the A-PVA aqueous solution with or without following annealing at 180 °C for 10 min in an argon atmosphere [15]. According to the previous assignment [7–11,14,15], these three components are assigned to the crystalline, less mobile noncrystalline and mobile noncrystalline components in the order of decreasing T_{1C} values, respectively. Here, the less mobile component may be subjected to some restriction in molecular mobility and conformation from the surfaces of the crystallites because the chain ends are connected to them, while the mobile component will be allowed not to strongly undergo such restriction from the surfaces. Interestingly, the T_{1C} values of the crystalline component are the smallest for the melt-crystallized sample, whereas the un-annealed films have the largest T_{1C}s for the component. Since the T_{1C} values of the crystalline component for polymers frequently depend on the crystallite size and the disordering in the crystallites, such a remarkable change in T_{1C} for A-PVA suggests that these parameters associated with crystallinity may be primarily affected by the temperature of the crystallization or annealing. In particular, the smallest T_{1C} value for the melt-crystallized sample is mainly due to the higher molecular mobility as a result of the preferable formation of the intramolecular hydrogen bonding in this sample as described later.

As for the noncrystalline components, their T_{1C} values for the melt-crystallized sample are found to be remarkably smaller than those of the un-annealed and annealed films although there is no significant difference in T_{1C} between the latter two films. It is well known that smaller T_{1C} values for the noncrystalline components imply more enhanced molecular motion with rates corresponding to the resonance frequency under the present experimental condition. Therefore, the molecular mobility of the noncrystalline chains is much more enhanced for the melt-crystallized sample compared to the cases of the un-annealed and annealed samples. This fact suggests that motional restrictions induced for the noncrystalline chains by the co-existing crystallites may be appreciably reduced in the former sample probably due to the process characteristic of the melt-crystallization as discussed later.

By using the differences in T_{1C}s thus revealed between the crystalline and noncrystalline components, the ^{13}C NMR spectra for these two components of the melt-crystallized sample were obtained as previously reported [7–11,14,15]. Here, the spectrum of the crystalline component, which is shown in Fig. 1(b), was selectively measured by the CPT1 pulse sequence by setting the delay time τ to 35 s, because the two noncrystalline components disappear at τ=35 s. On the other hand, the spectrum of the noncrystalline component, which contains the two noncrystalline components with different T_{1C}s, was obtained by subtracting the crystalline component from the total spectrum as shown in Fig. 1(c). As is already described, the CH resonance line of the crystalline component splits into lines I, II and III due to the formation of two, one and no intramolecular hydrogen bond(s) in the triad sequences with the planar zigzag conformation, respectively [7–11,14,15,18]. In contrast, the CH resonance line for the noncrystalline component seems to contain additional contributions together with lines I, II and III and the relative intensities of the latter three lines may greatly differ from those for the crystalline component. This fact suggests that the spectrum of the noncrystalline component may reflect some

Table 1
^{13}C spin–lattice relaxation times of the resonance lines for different A-PVA samples, measured at room temperature

Samples	T_{1C}/s											
	CH									CH_2		
	I′			II′			III′					
Un-annealed[a]	72.8	7.9	–[b]	69.0	14.4	2.8	61.9	12.2	2.6	68.0	11.3	0.7
Annealed[c]	56.3	7.2	–[b]	59.5	15.4	4.7	65.2	14.7	3.4	65.1	12.4	1.9
Melt-crystallized	35.1	4.3	–[b]	38.2	7.4	0.9	39.3	6.9	1.3	36.0	5.5	1.2

[a] Prepared at room temperature by casting from the 6% aqueous solution [15].
[b] Not estimated because of the low signal/noise ratio.
[c] The un-annealed films[a] were annealed at 180 °C for 10 min in an argon atmosphere [15].

influences due to the appearance of the *gauche* conformations, which produces an appreciable upfield shift of a specific resonance line as is well known as the γ-*gauche* effect [19], and the resulting formation of the intramolecular hydrogen bonding which induces a marked downfield shift [7,13].

We have already developed the analytical method of the spectra of the crystalline and noncrystalline component in different PVA samples [13]. In this analysis, two major shifts of the ^{13}C chemical shift values are evaluated, which are induced by the so-called γ-*gauche* effect produced by the carbon or oxygen nuclei at the γ position [19,20] and the formation of intramolecular hydrogen bonding in the triad sequences with different tacticities and conformations. Finally, nine resonance lines with different chemical shifts are found to theoretically exist for the CH carbons depending on the differences in tacticities, conformation and intramolecular hydrogen bonding, and numerical equations for the relative intensities of these lines are also derived as functions of the triad tacticities, the probability f_t for the *trans* conformation in each C–C bond and another probability f_a for the formation of the intramolecular hydrogen bonding in the possible *m* or *r* units [13].

Fig. 3 shows the results of the lineshape analyses using nine constituent lines described above for the CH resonance lines of the crystalline and noncrystalline components shown in Fig. 1(b) and 1(c), respectively. Here, each constituent line is assumed to be described as a Gaussian curve. As is clearly seen in Fig. 3(a), the composite curve (broken line) of lines 1, 3 and 6, which respectively correspond to lines I, II and III, is in good accord with the observed curve (thick solid line) for the crystalline component although a minor Gaussian contribution denoted as line III_f should be introduced most upfield. Such good fitting is highly reasonable as a result of the reflection of the fact that each PVA chain has the planar zigzag conformation in the crystalline region [21,22]. In addition, line III_f, which is assigned to the CH carbons bonded to the OH groups free from hydrogen bonding [23], is also observed for the crystalline component in the hydrated or uniaxially drawn A-PVA samples [7,10,11]. In contrast, lines 2, 4, 5 and 8 should be introduced in addition to lines 1, 3, and 6 to obtain good fitting for the noncrystalline component, as shown in Fig. 3(b). Since the former four lines are associated with the *gauche* conformation, this fact indicates that some amount of the *gauche* conformation is really produced in the noncrystalline region.

As described above, the integrated intensities of the respective constituent lines for the CH resonance lines in the crystalline or noncrystalline component can be calculated by using the equations previously derived [15]. In this case, it is assumed according to the previous evaluation [15] that almost no preferential partitioning of the *mm*, *mr* and *rr* sequences may occur in the crystalline and noncrystalline regions at least in the case of A-PVA. Fig. 4 shows the experimental integrated intensities (solid histograms) for the constituent lines obtained by the lineshape analysis shown in Fig. 3 and the statistically calculated intensities (open histograms) that were obtained so as to fit the experimental intensities by the least-squares method by using the f_t and f_a values as adjustable parameters. The calculated intensities are in good accord with the experimental intensities for both crystalline and noncrystalline components. This fact supports the assumptions that the intra- and inter-molecular hydrogen bonds are statistically formed in each component and the *trans* and *gauche* conformations are almost randomly distributed along the A-PVA chains in the noncrystalline component.

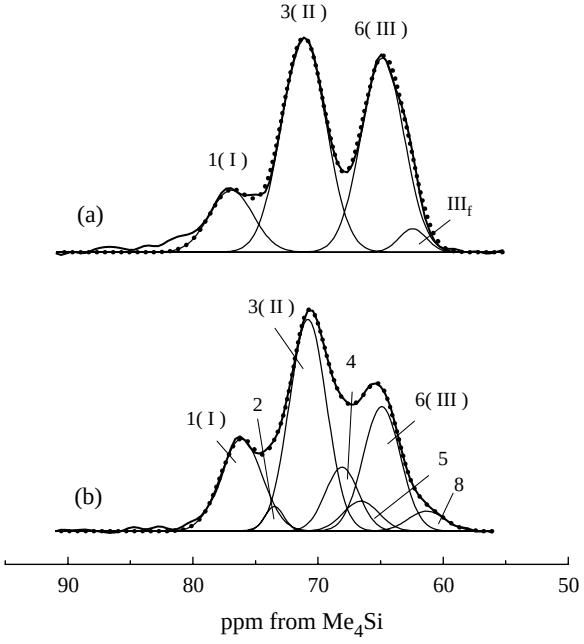

Fig. 3. Line shape analysis for the CH resonance line of each component for the melt-crystallized PVA films: (a) crystalline, (b) noncrystalline. The broken line indicates the composite curve of the constituent lines shown by thin solid lines.

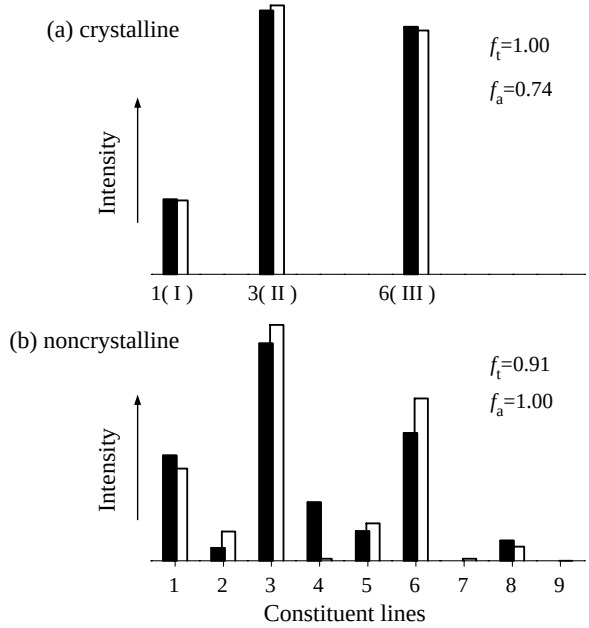

Fig. 4. Histograms for the observed and calculated relative intensities of the nine constituent lines of each component for the melt-crystallized PVA films: (a) crystalline, (b) noncrystalline.

It should be additionally noted here that the disagreement between the observed and calculated intensities is appreciably large for line 4 for the noncrystalline component as seen in Fig. 4(b). If the f_t value is significantly reduced from 0.91, the calculated intensity of line 4 is considerably increased resulting in the better fitting for line 4. However, it is not a good way in this case because the disagreements of the other lines become seriously large. It is, therefore, plausible to evaluate the contribution of line 4 separately from the other lines. According to the definition of line 4[13] this line should be assigned to the central CH carbon in the CH(OH)–CH_2–CH(OH)–CH_2–CH(OH) sequence adopting the g^+ttg^- or g^-ttg^+ conformation without intramolecular hydrogen bonding at high f_t values. Here, g^+, t, and g^- indicate *gauche*$^+$, *trans*, and *gauche*$^-$, respectively. It is, therefore, pointed out that line 4 should be the contribution from the folding parts of the PVA chains and such a type of chain folding is not well described at high f_t values by the statistically random treatment that is successfully applicable to other parts of the noncrystalline chains as described above. More detailed discussion will be made in near future after obtaining more information by using different PVA samples.

The optimum f_t and f_a values thus obtained for the crystalline and noncrystalline components are shown in Table 2 together with the corresponding values previously reported for the un-annealed and annealed films [15]. Interestingly, the f_a values for both of the crystalline and noncrystalline components are found to appreciably increase in the order of the un-annealed, annealed and melt-crystallized samples, although the values are much larger for the noncrystalline component than those for the crystalline component. This fact suggests that intramolecular hydrogen bonding may be preferably formed at higher temperatures in both crystalline and noncrystalline regions. In contrast, no significant change in f_t is observed for the noncrystalline component among these samples and their values are as large as about 0.9 probably reflecting the locally extended chains of A-PVA.

3.2. Crystallization from the melt or from the aqueous solution for A-PVA

In the recent investigation of the melt-crystallization of A-PVA, the typical spherulitic morphology with a maltese was found to be formed and many stacked lamellae were also observed by transmission electron microscopy although they were irregularly stacked unlike the cases of polyethylene and isotactic polypropylene [6]. The thickness of the largest lamellae is about 24 nm, which is nearly twice of that of the solution grown single crystals [24,25], but it is much smaller than the maximum thickness of polyethylene or isotactic polypropylene crystallized in the hexagonal or mobile phase, respectively [26]. Moreover, the distribution of the lamellar thickness is not very broad compared to the latter two cases. It was, therefore, concluded that the chain sliding diffusion which induces lamellar thickening is relatively suppressed during the crystallization of A-PVA probably due to intermolecular hydrogen bonding.

Table 2
The probabilities f_a and f_t for the formation of intramolecular hydrogen bonding and for the *trans* conformation in each component for different A-PVA samples, respectively

Samples	Crystalline		Noncrystalline	
	f_a	f_t	f_a	f_t
Un-annealed[a]	0.56	1.0	0.85	0.89
Annealed[b]	0.67	1.0	0.97	0.92
Melt-crystallized	0.74	1.0	1.0	0.91

[a] Prepared at room temperature by casting from the 6% aqueous solution [15].
[b] The un-annealed films[a] were annealed at 180 °C for 10 min in an argon atmosphere [15].

According to the present experimental results described above, the f_a value for the crystalline component is appreciably larger for the melt-crystallized sample than that for the un-annealed or annealed sample prepared from the aqueous solution, but this value is still as low as 0.74 at room temperature although f_a may be generally increased at higher temperatures [11]. This indicates that intermolecular hydrogen bonding will still affect the melt-crystallization, as pointed out in the previous report [6], but the weight of the conventional van der Waals interaction must be increased for the A-PVA chains in the melt as a result of more frequent formation of intramolecular hydrogen bonding. Since the increase in crystallization temperature preferably induces the increase in f_a, the melt-crystallization at appropriately higher temperatures, under an applied pressure if necessary, will proceed without the effect of intermolecular hydrogen bonding in principle. However, such crystallization may be almost impossible because more serious thermal degradation will occur for A-PVA.

Another way to reduce the effect of intermolecular hydrogen bonding on the melt-crystallization is the introduction of the ethylene units to the PVA main chains, which corresponds to the use of ethylene–vinyl alcohol random copolymers. Recently, we have characterized intra- and inter-molecular hydrogen bonding of the copolymers as a function of the ethylene content and found that the f_a value approaches to 1.0 at an ethylene content of about 0.6 [27], where the pseudo hexagonal phase appears [28]. Therefore, in the copolymers with the ethylene contents of about 0.6–0.8, the crystallization seems to proceed without the significant effect of intermolecular hydrogen bonding and this fact may be closely associated with the appearance of the pseudo hexagonal phase in which each chain with the planar zigzag conformation is independently packed in the respective unit cells. The detail will be published somewhere in near future.

On the other hand, the crystallization occurring during the preparation of the films from the aqueous solution by casting at room temperature seems to basically correspond to the crystallization at a lower temperature in the presence of water. Since the f_a value is as low as 0.56 for the crystalline component of the un-annealed sample, the role of the intermolecular hydrogen bonding may be much more important in the crystallization. Probably the nucleation of the crystals will be induced by the formation of the

intermolecular hydrogen bonding among some PVA chains and the following crystal growth may be also mainly promoted through the intermolecular hydrogen bonding. Moreover, the intermolecular hydrogen bonding formed in such a way seems not to be readily reorganized during the crystallization and, therefore, some OH groups will be unable to take part in any hydrogen bonding in the crystallization. In fact, the mole fraction f_{IIIf} of the CH carbons bonded to the OH groups free from any hydrogen bonding is significantly higher in this system than that in the melt-crystallization: $f_{\mathrm{IIIf}}=0.08$ for the former [23] and $f_{\mathrm{IIIf}}=0.03$ for the latter as seen in Fig. 3.

Finally, the difference in the crystalline–noncrystalline structure produced through each crystallization should be briefly discussed: As pointed out above on the basis of the $T_{1\mathrm{C}}$ values shown in Table 1, molecular mobility of the noncrystalline chains is much enhanced for the melt-crystallized sample than for the un-annealed sample prepared from the aqueous solution and this fact may be due to the significant reduction of the motional restrictions induced by the co-existing crystallites for the former sample. Such a difference in the crystalline–noncrystalline structure is interpreted as follows by considering the difference in crystallization between two cases: in the melt-crystallization, reorganization of the aggregated chains in the crystalline nuclei to a more structurally stable state will be allowed for each chain as a result of the reduction of the influence of the intermolecular hydrogen bonding. Such a state may be somewhat close to the pseudo equilibrium state between the melt and crystalline phases. Moreover, the structural restriction for the folded noncrystalline segments that may be produced by the lateral crystal growth will be significantly relaxed by the crystal growth along the chain axis. These processes seem to allow the noncrystalline chains to adopt less restricted conformations, resulting in their more enhanced molecular mobility, for the melt-crystallized sample.

In contrast, the intermolecular hydrogen bonding preferably produced will significantly restrict the structural rearrangement in the crystalline nuclei in the crystallization for the un-annealed sample. Since such restriction in the rearrangement may appreciably suppress the crystal growth along the chain axis, many small and immature crystallites are produced and the noncrystalline chains are considerably restricted in conformation and molecular mobility by those co-existing crystallites. Therefore, the phase separation into the crystalline and noncrystalline phases seems relatively unclear in the un-annealed sample. In addition, it should be noted that such unclearly phase-separated structure is not greatly changed by annealing at 180 °C. This fact may be also due to the difficulty of the rearrangement of the intermolecular hydrogen bonding at lower temperatures.

Acknowledgements

This work was supported by Grand-in-Aid for JSPS Research by the Ministry of Education, Science, Sports and Culture of Japan.

References

[1] Sakurada I. Polyvinyl alcohol fibers. New York: Marcel Dekker; 1985 p. 115.
[2] Finch CA, editor. Polyvinyl alcohol-developments. Chichester, England: Wiley; 1992.
[3] Takahashi Y. J Polym Sci, Polym Phys 1997;35:193.
[4] Assender HE, Windle AH. Polymer 1998;39:4295.
[5] Assender HE, Windle AH. Polymer 1998;39:4303.
[6] Endo R, Amiya S, Hikosaka M. J Macromol Sci Phys 2003;B42:793.
[7] Horii F, Hu S, Ito T, Kitamaru R, Matuzawa S, Yamaura K. Polymer 1992;33:2299.
[8] Hu S, Tsuji M, Horii F. Polymer 1994;35:9516.
[9] Hu S, Horii F, Odani H. Bull Inst Chem Res, Kyoto Univ 1991;69:165.
[10] Hu S, Horii F, Odani H, Narukawa S, Akiyama A, Kajitani K. Kobunshi Ronbunshu 1992;49:361.
[11] Hu, S. PhD Dissertation. Japan: Kyoto University; 1991.
[12] Horii F, Masuda K, Kaji H. Macromolecules 1997;30:2519.
[13] Masuda K, Horii F. Macromolecules 1998;31:5810.
[14] Horii F, Masuda K. In: Ando I, Asakura T, editors. Solid state NMR of polymers. Studies in physical and theoretical chemistry, vol. 84. Amsterdam: Elsevier Biomedical; 1998. p. 713.
[15] Masuda K, Kaji H, Horii F. J Polym Sci Polym Phys 2000;38:1.
[16] Horii F, Hirai A, Kitamaru R, Sakurada I. Cellulose Chem Technol 1985; 19:513.
[17] Torchia DA. J Magn Reson 1981;44:117.
[18] Terao T, Maeda S, Saika A. Macromolecules 1983;16:1535.
[19] Tonelli AE. NMR spectroscopy and polymer microstructure: the conformation connection. New York: VCH; 1989.
[20] Born R, Spiess HW. Ab initio calculations of conformational effects on ^{13}C NMR spectra of amorphous polymers. Berlin: Springer; 1997.
[21] Bunn CW. Nature 1948;161:929.
[22] Sakurada I, Futino K, Okada N. Bull Inst Chem Res, Kyoto Univ 1950; 23:78.
[23] Masuda K, Kaji H, Horii F. Polym J 2001;33:356.
[24] Tsuboi K, Mochizuki T. Kobunshi Kagaku 1966;23:636.
[25] Tsuboi K, Mochizuki T. Kobunshi Kagaku 1967;24:241.
[26] Maiti P, Hikosaka M, Yamada K, Toda A, Gu F. Macromolecules 2000; 33:9069.
[27] Nishimura T, Kaji H, Horii F. Polym Prepr, Jpn 2003;52:1729.
[28] Takahashi M, Tashiro K, Amiya S. Macromolecules 1999;32:5860.